Brunacci, N.; Wischke, C.; Naolou, T.; Patzelt, A.; Lademann, J.; Neffe, A.; Lendlein, A.:

Formulation of drug-loaded oligodepsipeptide particles with submicron size.

In: Clinical Hemorheology and Microcirculation. Vol. 77 (2021) 2, 201 - 219.
First published online by IOS: 19.03.2021

https://dx.doi.org/10.3233/CH-200977

Title: Formulation of drug-loaded oligodepsipeptide particles with submicron size

Authors: Nadia Brunacci[1,2], Christian Wischke[1], Toufik Naolou[1], Alexa Patzelt[3], Jürgen Lademann[3], Axel T. Neffe[1], Andreas Lendlein[1,2]*

[1]Institute of Biomaterial Science and Berlin-Brandenburg Centre for Regenerative Therapies, Helmholtz-Zentrum Geesthacht, Teltow, Germany;
[2]Institute of Chemistry, University of Potsdam, Potsdam, Germany;
[3]Charité – Universitätsmedizin Berlin, corporate member of Freie Universität Berlin, Humboldt-Universität zu Berlin, and Berlin Institute of Health, Department of Dermatology Venereology and Allergology, Center of Experimental and Applied Cutaneous Physiology, Berlin, Germany.
*: Corresponding author, email: andreas.lendlein@hzg.de

Abstract:

The size of particulate carriers is key to their transport and distribution in biological systems, and needs to be tailored in the higher submicron range to enable follicular uptake for dermal treatment. Oligodepsipeptides are promising nanoparticulate carrier systems as they can be designed to exhibit enhanced interaction with drug molecules. Here, a fabrication scheme for drug-loaded submicron particles from oligo[3-(*S*)-*sec*-butylmorpholine-2,5-dione]diol (OBMD) is presented based on an emulsion solvent evaporation method with cosolvent, surfactant, and polymer concentration as variable process parameters. The particle size (300-950 nm) increased with lower surfactant concentration and higher oligomer concentration. The addition of acetone increased the particle size at low surfactant concentration. Particle size remained stable upon the encapsulation of models compounds dexamethasone (DXM) and Nile red (NR), having different physicochemical properties. DXM was released faster compared to NR due to its higher water solubility. Overall, the results indicated that both drug-loading and

size control of OBMD submicron particles can be achieved. When applied on porcine ear skin samples, the NR-loaded particles have been shown to allow NR penetration into the hair follicle and the depth reached with the 300 nm particles was comparable to the one reached with the cream formulation. A potential benefit of the particles compared to a cream is their sustained release profile.

Keywords: Submicron particles, oligodepsipeptide, formulation parameters, emulsion solvent evaporation, surfactant, release kinetics

Introduction:

Polymer particles offer opportunities for encapsulation, transport and/or release of payload for medical applications, especially for drug delivery and diagnostics. The mobility of particles, which comprises their transport in the body, distribution in a tissue, and crossing of biological barriers such as the skin, mucosae, cell membranes, as well as blood/tissue- or blood/brain-barriers, is typically a function of the particle size and geometry. In the case of skin delivery, the outermost skin layer, the stratum corneum, hinders the penetration of most molecules across the skin. It has been reported that skin penetration can be enhanced by using nanoparticles that can deform or dynamically reorganise and can interact with skin structures, such as the skin lipids [1]. An alternative skin delivery pathway is represented by the hair follicles, which can act as drug reservoir and penetration shunts, thus increasing the absorption of topically applied substances [2]. A size-dependent penetration of particles of 120 to 860 nm into the hair follicle of healthy skin has been shown, with the deepest penetration observed by particles of approximately 640 nm [3]. Moreover, different structures of the terminal hair follicle could be selectively targeted by using the following mean particle sizes: particles of 120 nm and of 860 nm to target the infundibular region, particles of 230 nm and 300 nm to reach the sebaceous gland, and 470 and 643 nm particles to treat the bulge region [3]. It should be noted that particles directed towards the follicular uptake are distinctly larger than particles crossing other barriers. Those particles are typically in the nano- or lower submicron size range and aim e.g. at exploiting the postulated enhanced permeation and retention (EPR) effect in cancer treatment [4] and allow topical delivery in ocular, pulmonary or dermal diseases [3,5-8]. For example, in the case of ophthalmic applications, particle diameters from 50 to 400 nm are preferred as they enhance the drug penetration and are better tolerated by the patients compared

to bigger particles [9-13], improving the treatment of diseases of the anterior and posterior ocular segments [13].

The size of polymer particles, together with other parameters such as the polymer degradation behavior, influences also the release profile of the encapsulated drug. By default, a release governed by diffusion is faster from particles of smaller size than of that of larger sizes, as the required diffusion distance is shorter [14].

As the particle size strongly influences its uptake pathway and distribution, a narrow size distribution is requried to favor a desired uptake, thereby promoting delivery of the load to the desired side and avoiding accumulation in other locations [15]. Among the drugs that have been encapsulated in nanoparticulate carriers, the clinically relevant glucocorticoid dexamethasone (DXM) is one of the most widely investigated as it is frequently used to treat inflammatory diseases, especially for ocular and skin applications [16,17].

When aiming to tailor the functional performance of carriers systems, particularly such material platforms that offer structural variety that can be exploited to increase interactions or change physicochemical properties are of interest. One example for such a material platform are oligodepsipeptides (ODPs). These copolymers are composed of alternating α-hydroxy and α-amino acids. Similar to polypeptides and β-peptides, their properties can be tailored by changing the structure of their side chains [18,19]. In hydrolytic degradation, ODPs do not lower the pH value [20] as was observed in the case of poly[(*rac*-lactide)-*co*-glycolide] (PLGA) [21]. So far, *in vitro* and *in vivo* studies have shown a beneficial compatibility profile of depsipeptides and their copolymers [22-24]. Their unique repetitive structural features comprising both amide and ester bonds in their backbone can establish inter- and intra-chain hydrogen bonds that may promote the stabilization of the final carrier systems [24,25] and potentially enhance interactions with other molecules, e.g drugs. Drug-loaded nanoparticles

(~150 nm) from oligo[3-(*S*)-*sec*-butylmorpholine-2,5-dione]diol (OBMD) showed a drug loading (DL) one order of magnitude higher than PLGA nanoparticles [20]. Modelling and experimental studies demonstrated that this effect could be explained by enhanced drug-OBMD interaction, as rationalized by both hydrogen bond donors and acceptors availability in ODPs compared to polyesters providing only hydrogen bond acceptor moieties. ODP copolymers with low depsipeptide content have been more extensively studied than ODP homopolymers due the limited availability of morpholindione monomers. They have been explored for several biomedical applications [26] including porous sponges enabling cell growth [19] or for drug [27] and gene delivery [24]. Furthermore, drug-loaded nanoparticles in a size range of 150-350 nm prepared from a copolymer consisting of L-lactide and glycolide-L-leucine repeating units have been reported [27]. Progress in synthesis and upscaling [28,29] allows now employing ODP homopolymers. In recent work, first pure ODP submicron particles were introduced. Drug-loaded particles with diameter of ~130-170 nm were obtained from a ODP homooligomer by nanoprecipitation [20]. In terms of broaden the scope of applicability such as delivery to the skin, potentially exploiting follicular uptake, larger particles would be required. By choosing a suitable surfactant, size control of OBMD submicron particles in the range of 300 to 900 nm principally has shown to be possible using a solvent emulsion evaporation method [30]. However, that study was limited to unloaded particles and the encapsulation of drug molecules was not investigated.

The emulsion solvent evaporation technique is one of the most common procedures used to prepare polymer particles starting from previously synthesized polymers [31-33]. In this method, the polymer is dissolved in a volatile, non-water miscible solvent and an emulsion is prepared by dispersing it in a non-solvent, which is commonly water. A surfactant is typically added to stabilize the emulsion as well as the particles

after hardening. It has been demonstrated by several studies that this method allows the formation of particles in the submicron size range when it was applied to different polymeric materials, such as polyesters and polyamides [34,35]. Moreover, the size of polymeric particles can be tailored by varying the formulations parameters. In the case of polyester based particles, for example, an increase in the particle size is often obtained by increasing the polymer concentration [27,36-38] or decreasing the surfactant concentration [27,39-41]. In both cases, the larger particle size has been attributed to an increase of the emulsion droplet size, as result of a more viscous organic phase in the case of higher polymer concentration [38] or a decrease of the emulsion stabilization in the case of lower surfactant concentration [41]. However, an increase of the surfactant concentration may also be associated with the formation of larger particles due to an increase of the viscosity of the aqueous phase [38,42,43]. The addition of water miscible cosolvents in the organic phase may result in smaller particles as shown in the case of polyester-based particles [44-46]. It has been postulated that the reduction in the interfacial tension between the organic and aqueous phase promotes the formation of smaller droplets during emulsification and, therefore, smaller sized particles [46]. It has also been hypothesized that the fast diffusion of the cosolvent from the emulsion droplets to the aqueous phase would lead to a reduction of the size of the droplets, and hence resulting in smaller particle size [44]. Moreover, the presence of a cosolvent has been demonstrated to affect the particles drug loading (DL) [46-49]. The exact influence depends on the polymer, solvent, and cosolvent, as increased solubility of the drug in the mixed aqueous/cosolvent phase may reduce DL [46], while fast cosolvent diffusion leading to rapid polymer precipitation has been reported to increase DL [49]. The presence of a cosolvent furthermore affected the initial state of the payload to be either dispersed (solid-in-oil-in-water, s/o/w) or dissolved (oil-in-water, o/w) in the organic polymer

phase. While in the case of polyesters many studies have been performed, the knowledge about the possibility of tailoring the size of particles from ODPs is limited to ODP copolymers [27] or to unloaded particles [30].

In this study, the aim was to tailor the size of drug-loaded submicron particles from ODP homopolymers in a wide but narrowly defined submicron range and with a similar drug loading in order to extend ODP use to several clinical applications, especially skin delivery via the follicular pathway. It was hypothesized that such ODP particles could be prepared by emulsion solvent evaporation by systematically varying several formulation parameters. Consistently used were DXM as model drug with applicability in treatment of skin diseases such as psoriasis and atopic dermatitis and Nile red (NR) as more hydrophobic model payload that has furthermore relevance for particle visualization in tissues. Particles of similar sizes loaded with DXM and NR could then potentially be used to study the particle penetration inside the hair follicles. Considering that *ex vivo* skin penetration studies are usually performed in a time range of 30 min – 1 hour [3,50,51], a payload release profile extending for at least 1 hour was targeted. As organic solvent, chloroform was employed as it has low water solubility and is easily evaporated, as required in the particle preparation. Four-armed star-shaped oligo(ethylene glycol) of molecular mass of 10 $kg \cdot mol^{-1}$ functionalized with desamino-tyrosine (sOEG-DAT) has been used as surfactant [30]. The varied parameters were surfactant concentration, polymer concentration, and the presence of acetone as cosolvent. In addition, the influence of the two different encapsulated molecules (DXM and NR) on the release kinetics obtained from the loaded particles was examined.

Materials and methods:

Materials

Oligo[3-(*S*)-*sec*-butylmorpholine-2,5-dione]diol (OBMD) ($M_{n(NMR)}$ = 4.7 kg·mol^{-1}, PDI = 1.2) was synthesized via ring opening polymerization according to Ref. [28]. Four-armed star-shaped oligo(ethylene glycol) ($M_{n(Maldi\text{-}TOF)}$ 10.2 kg·mol^{-1}) was functionalized with desaminotyrosine (Sigma-Aldrich GmbH, Schnelldorf, Germany) (sOEG-DAT) (degree of functionalization (d.f.) = 69%) according to Ref. [52]. Nile red (NR) and dexamethasone (DXM) (≥98% (HPLC), powder, T_m = 262-264 °C) were from Sigma-Aldrich (Schnelldorf, Germany). Acetone (≥99.5%) was bought from Sigma-Aldrich (Steinheim, Germany) and chloroform (99%) was obtained from Roth (Karlsruhe, Germany). Phosphate buffered saline (PBS) (pH 7.4, 1X) was purchased from Thermo Fisher Scientific (Schwerte, Germany).

Methods

Particle preparation by emulsion - solvent evaporation method

A single oil-in-water emulsion process followed by solvent evaporation was employed to prepare unloaded, DXM- and NR-loaded OBMD particles. OBMD (5–20 mg) was dissolved in 1 mL of chloroform and added dropwise into 5 mL of aqueous surfactant solution (0.1–1 wt.% sOEG-DAT). In the case of acetone as cosolvent, the volume of the organic phase was kept constant, and was a mixture of chloroform and acetone (exact compositions see Table 1). The two phases were mixed at 25,000 rpm for 90 s using a T 25 digital ultra-turrax with a 10 G dispersing tool (IKA GmbH, Königswinter, Germany). Afterwards, the emulsion was sonicated for 2 min with an intensity of 52% using a Bandelin Sonoplus sonicator HD 3200 with a T61 probe (Bandelin Electronic GmbH & Co. KG, Berlin, Germany). The emulsion was poured in a beaker containing 5 mL of identical surfactant solution and stirred for solvent evaporation (r.t., 300 rpm, 5 h). The suspension was filtrated (40 µm nylon cell strainer, neoLab GmbH, Heidelberg, Germany) to remove aggregates formed during solvent evaporation. To

prepare DXM- and NR-loaded particles, the oligomer solution was supplemented with DXM (2 mg) or NR (0.1 mg) dissolved in acetone (0.2 - 0.4 mL) prior to particle preparation. Alternatively, a solid-in-oil-in-water with dispersed DXM powder was evaluated. All experiments were repeated at least in triplicate.

Particle size characterization

The particle size (D_h) and the polydispersity index (PDI) of the particle suspension were determined in aqueous dispersion at 25 °C by Dynamic Light Scattering (DLS) using ZetasizerNano SZ (Malvern, Worcestershire, UK). Each sample was measured three times with 10 sub-runs each time.

Quantification of drug loading

2 mL of the particle suspension was centrifuged; the pellet was then washed with water (2 mL), centrifuged again and lyophilized. The dried, balanced particles were dissolved in 0.6 mL of acetonitrile. The polymer was precipitated by adding water (1.4 mL), while keeping DXM dissolved in the supernatant. After centrifugation, dissolved DXM was quantified by High-Performance Liquid Chromatography (HPLC) using a Dionex Ultimate 3000 system (Dionex Softron GmbH, Germering, Germany) with UV detection (240 nm). A LiChrospher® 100 RP-18 (5 µm) LiChroCART® 125-4 (Merck Chemicals GmbH, Darmstadt, Germany) column was used. The mobile phase consisted of a 65:35 vol./vol.% mixture of water, which contained 0.1 vol.% TFA in solution, and 35 vol.% acetonitrile. Analyses were performed at a flow of 1 $mL \cdot min^{-1}$.

The amount of NR in the particles was determined by UV/Vis spectrophotometry using a Tecan Infinite F50 (Tecan Deutschland GmbH, Crailsheim, Germany) microplate reader and analyzing the solution at $\lambda = 560$ nm.

The drug/dye loading (DL%) was calculated according to eq. (1).

$$\text{DL}\ (\%) = \frac{\text{Mass of drug/dye encapsulated}}{\text{Mass of loaded particles}} \cdot 100 \quad (1)$$

In vitro release kinetics

In vitro release studies of DXM-loaded particle suspension (1.5 mL) of known concentration were performed by dialysis using Pur-A-Lyzer maxi dialysis membrane (regenerated cellulose, cut off 50 $kg \cdot mol^{-1}$) at 32 °C, mimicking skin surface temperature and ensuring sink conditions (12 mL of phosphate buffer saline (PBS, pH 7.4)). Samples were on an orbital shaker (600 rpm, DITABIS, Pforzheim, Germany), from which 2 mL of medium was collected for sampling and replaced with fresh PBS. *In vitro* release studies of NR from the particles were performed in a similar manner, except that the entire release medium was collected for lyophilisation and replaced by fresh PBS at every time point to maintain sink conditions. The lyophilisate was dispersed in 0.7 mL water and three times extracted with 0.4 mL chloroform (10 min shaking). The organic phases were dried and NR was dissolved in 0.3 mL of DMSO and quantified by UV/Vis spectrophotometry.

Ex vivo follicular penetration study

The *ex vivo* follicular penetration study was performed on fresh porcine ear skin, which was obtained from a local butcher and stored in the refrigerator for less than 3 days. The skin was thoroughly washed with distilled water, dried, and the hairs were trimmed using a pair of scissors. To prevent lateral diffusion of the colloidal dispersion, an adhesive solution was put around the application area (2 cm × 3 cm) and dried for 90 min. Then, 50 µL of the particle suspension was uniformly spread over the application areas (n=3). Particles of two sizes were used: 625±7 nm with a PDI = 0.237 (0.86 $mg \cdot mL^{-1}$ suspension in water, with a loading of 0.86 mg NR per 100 mg particles, prepared by the formulation protocol NR-1-0.1-20) and 258±1 nm with a PDI = 0.072

(0.915 mg·mL^{-1} suspension in water, with a loading of 0.88 mg NR per 100 mg particles, prepared by the formulation protocol NR-1-0.5-20). This corresponds to a NR concentration of 0.007-0.008 wt%. For comparison, 50 µL of an oil-in-water cream (Basiscreme DAC, German Pharmacopoeia) with a NR loading of 0.0075 wt% was used. The so treated skin was incubated at 35 °C for 1 h. Then, cryo spray was applied and biopsies of about 0.6 cm × 0.6 cm were cut out using a scalpel. The biopsies were put in an Eppendorf tube, frozen in liquid nitrogen and stored at -20 °C. Finally, the biopsies were mounted in a frozen tissue freezing medium and 10 nm histological sections containing hair follicles (n = 10) were cut out using a cryostat (Microm HM 560, Microm GmbH, Walldorf, Germany) and observed under a CLSM (LSM 410, Zeiss; Berlin, Germany) to record the penetration depth of NR. Digital images and measurements of the penetration depths were obtained using the software LSM 410 Invert Basic, v.3.98 (Zeiss). The fluorescent probes were excited using an argon ion laser with a wavelength of 488 nm. As skin exhibits autofluorescence between the wavelengths of 520 and 560 nm, emission signals were detected with the FT 589 dichroic beam splitter and long pass filter LP 590 to exclude any autofluorescence effects. The depths of fluorescence detection were determined from the skin surface to the deepest maximum signal in the hair follicle. The experiments were authorized by the Commission of Consumer Protection and Agriculture, District Dahme-Spreewald, Germany.

Data analysis and statistical evaluation

Statistical evaluation was carried out by two-tail t-test (in the case of comparison between two groups) or one-way Anova analysis (in the case of comparison between three or more groups of data) using Graphpad Prism software for data sets with n≥3. Significant difference was concluded at a maximum p-value < 0.05, while the

determined values * $p < 0.05$, ** $p < 0.01$, *** $p < 0.001$, and **** $p < 0.0001$. If not specified differently, data are shown as average value ± standard deviation (SD).

Results and discussion:

In order to investigate the preparation of ODPs submicron particles in a wide size range that could be used for different clinical applications, emulsion solvent evaporation has been chosen. The influence of four formulation parameters, i.e. surfactant concentration, oligomer concentration, the presence of acetone as cosolvent, and type of payload, on the size and drug/dye loading of OBMD particles has been explored, as shown in Fig. 1.

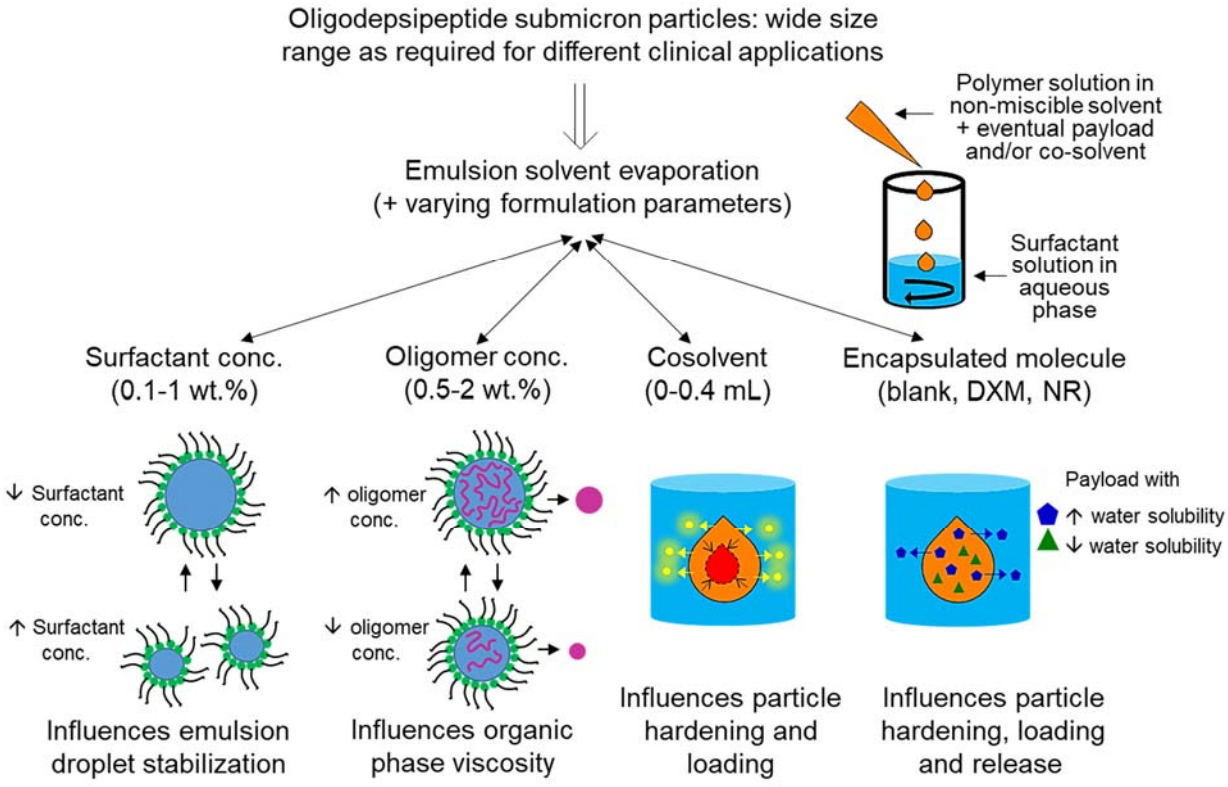

Fig. 1: Fabrication scheme that illustrates the experimental strategy that has been followed to investigate the preparation of ODPs submicron particles in a wide size range. An emulsion solvent evaporation method has been used and four formulation variables have been investigated: (i) the surfactant concentration, which influences the stabilization of the emulsion droplets (surfactants here depicted for simplicity as tenside with head-tail structure); (ii) the oligomer concentration, which defines the viscosity of the organic phase, (iii) the presence of a cosolvent that affects the particle hardening and loading, and (iv) the encapsulated molecule, which can determine the particle hardening, loading and cargo release.

The surfactant and the oligomer concentration have been systematically varied and the concentrations chosen in the present study were similar to the ones that led to the successful preparation of unloaded ODP particles in the submicron size range in a previous work [30]. The addition of acetone as water miscible cosolvent was investigated, as in studies regarding polyester-based particles, the addition of a cosolvent decreased the particle size and affected the particle DL [44-49]. As payloads, the clinically relevant anti-inflammatory drug DXM and the dye NR have been chosen. Sample codes and compositions are explained in Table 1.

Table 1: Formulation parameters varied for the preparation of unloaded, dexamethasone (DXM) and Nile red (NR) loaded particles.

Code	OBMD (wt.%)	sOEG-DAT (wt.%)	Acetone (Vol%)	Encapsulated molecule
DXM-1-**S**	1	**0.1, 0.2, 0.5, 1**	0	DXM
DXM-**D**-0.1	**0.5, 1, 1.5, 2**	0.1	0	DXM
DXM-1-0.1-**C**	1	0.1	**0, 20, 40**	DXM
DXM-1-0.5-**C**	1	0.5	**0, 20, 40**	DXM
P-1-0.1-20	1	0.1	20	**blank/ DXM/ NR**
P-1-0.5-20	1	0.5	20	**blank/ DXM/ NR**

Sample code: P-D-S-C with P defining the payload (blank = unloaded, DXM= dexamethasone-loaded, NR= Nile red-loaded), D defining the depsipeptides concentration in the organic phase, S defining the concentration of the surfactant sOEG-DAT in the water phase, C defining the volume % of acetone in the organic phase)

Influence of surfactant concentration

The effect of surfactant concentration (0.1, 0.2, 0.5 and 1 wt.% sOEG-DAT) on particle size and size distribution was determined while keeping the other three parameters constant (1 wt.% OBMD; no acetone; DXM payload). The D_h of the particles decreased significantly from 590 to 270 nm with increasing surfactant concentrations (Fig. 2), while high sOEG-DAT concentrations (1 wt.%) did not allow further size reduction. The inverse correlation of particle size and surfactant concentration is commonly attributed

to a higher availability and a faster interface saturation by surfactant allowing for advanced droplet stabilization. This effect is also visible by the reduction of the range of the particle's D_h obtained from independent batches of the same formulation (0.1 to 0.5 wt.% sOEG-DAT), indicating improved reproducibility and lower inter-batch variability when a higher surfactant concentration was used. However, high amounts of surfactant can increase the viscosity of the water phase, which hinders the formation of small stable organic droplets within the water phase and, therefore, is one parameter that sets limits to further particle size reductions. Similar results have been obtained for other systems, including a tendency in increasing particle sizes at very high surfactant concentrations [43,53,54]. In all four formulations investigated in this part of the study, the particle polydispersity was narrow and characterized by a polydispersity index (PDI) <0.25. Similar to the particle size, also the average PDI was slightly reduced when a more concentrated surfactant solution was used.

The particle size range that was obtained here (250-600 nm) was broader than the size range achieved in a previous study (150-270 nm), in which poly-(vinyl alcohol) (PVA) was used as surfactant of similar concentrations (0.1-1 wt.%) to prepare particles from a copolymer with L-lactide and glycolide-L-leucine repeating units [27]. In the case of rutin-loaded PLGA particles, an increase of the PVA concentration from 0.1 to 3 wt.% resulted in the reduction of the particles size from 646 to 212 nm, while, a further increase of the surfactant concentration to 5 wt.% increased the particles diameter to 570 nm [55]. Lamivudine-poly(ε-caprolactone) conjugate submicron particles showed a decrease in the diameter from 785 to 272 nm and a slightly smaller PDI when the PVA concentration was increased from 0.1 to 1.5 wt.%. A further increase to 2 wt.% resulted in slightly larger particles [41].

The DL was only slightly affected by the surfactant concentration: DL was 1.1 wt.% when the lowest sOEG-DAT concentration was used and it decreased to about

0.9 wt.% in the case of the other three surfactant concentrations (Tab. 2). This effect might be related to the increased solubility of the drug in the aqueous phase during particle preparation as promoted by the higher surfactant concentration [56,57]. The DL achieved was similar to the DL of DXM-loaded particulate carriers prepared from ethyl cellulose and/or poly[(ethyl acrylate)-*co*-(methyl methacrylate)-*co*-(trimethylammoniumethyl methacrylate chloride)] (Eudragit® RS), that were investigated for drug delivery to the skin and the corneal epithelium [58]. Such particles were prepared by the solvent evaporation method and showed a DL in the range of 0.3 – 2.2 wt.% depending on the formulation parameters chosen. The DL achieved here is also similar to the DL achieved in a previous study, in which DXM-loaded particles of about 150 nm prepared using a nanoprecipitation method had a DL of approx. 1-2 wt.% [20].

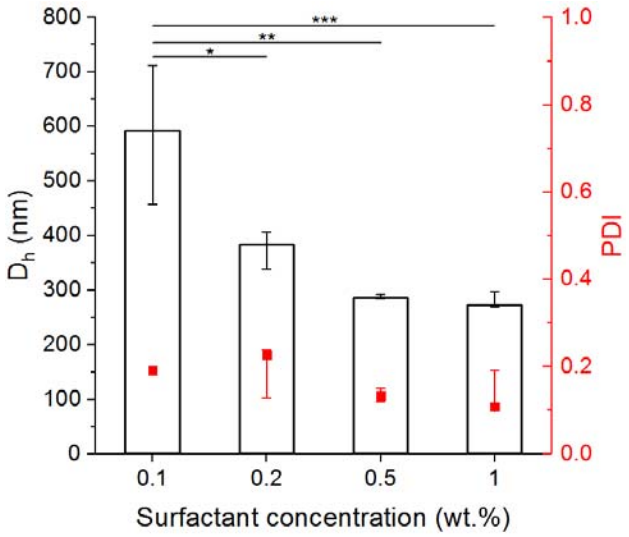

Fig. 2: DLS data of DXM-loaded OBMD particles obtained with formulations DXM-1-**S** characterized by different surfactant concentrations while maintaining oligomer concentration constant at 1 wt.%, without the addition of a cosolvent to the organic phase. The median and range (error bars) of at least three batches are shown. Bars indicate statistically significant different values with * $p < 0.05$, ** $p < 0.01$ and *** $p < 0.001$.

Table 2: DL data of DXM-loaded OBMD particles obtained with formulations DXM-1-**S** characterized by different surfactant concentrations while maintaining oligomer concentration constant at 1 wt.% and without the addition of a cosolvent to the organic phase. The value shown is the median of at least three batches with the corresponding range in brackets.

	DXM-1-0.1	DXM-1-0.2	DXM-1-0.5	DXM-1-1
DL (wt.%)	1.14 (0.91-1.33)	0.86 (0.81-0.88)	0.86 (0.83-1.06)	0.85 (0.84-0.96)

Influence of oligomer concentration

The influence of oligomer concentration on the particle size and DL was studied using formulations with sOEG-DAT solution of 0.1 wt.%, in absence of acetone as cosolvent and with DXM as embedded molecule. An almost linear relationship between increasing OBMD concentration (0.5 to 2 wt.% in chloroform) and increasing particle sizes was detected (Fig. 3), ranging from 370 up to 820 nm at narrow PDI of 0.18 - 0.22. The increase of the particle size upon the use of higher oligomer concentration has also been observed for other particulate systems [27,36,37,59] and is generally attributed to the increased viscosity of the organic phase, which results in larger droplets in the emulsion. However, in many studies that investigated PLGA-based carriers, the particle size increase was limited to less than 200 nm [55], even when different organic phases were used [60], or no influence of the PLGA concentration over the particle diameter was observed in the range studied [41,61].

The particles obtained from 0.5, 1 and 1.5 wt.% OBMD had a similar DL of 0.9 to 1.1 wt.% (see Table 3). The DL was reproducible within the different batches prepared for each formulation. On the contrary, the DL of the particles prepared with the oligomer concentration of 2 wt.% (DXM-2-0.1) showed both higher loading and higher variation in-between triplicates ranging from 1.7 to 3.3 wt.%. The higher DL at 2 wt.% OBMD might result from the increased probability of the OBMD-drug interaction supporting

drug encapsulation [20]. However, the broad range of values obtained suggests that interface kinetics, nascent particle solidification and drug loss during the multi-step dispersion process may not be strictly controllable, contributing to DL variation under this condition.

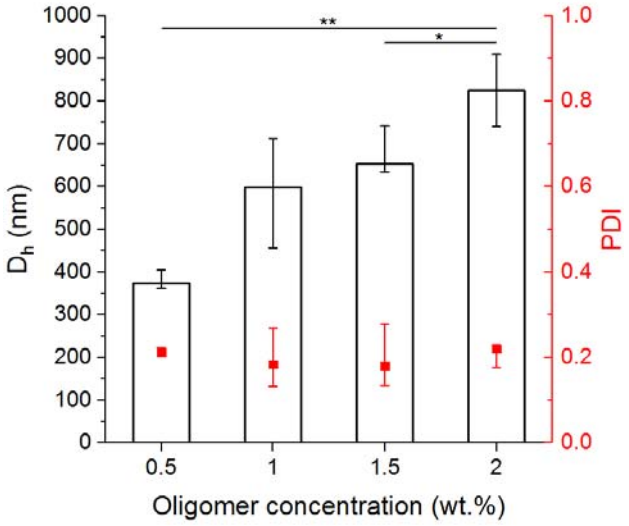

Fig. 3: DLS data of DXM-loaded OBMD particles obtained with formulations DXM-**D**-0.1 characterized by different oligomer concentrations, while maintaining the surfactant concentration constant at 0.1 wt.%, without the addition of a cosolvent to the organic phase. The median and range (error bars) of at least three batches are shown. Bars indicate statistically significant different values with * $p < 0.05$ and ** $p < 0.01$.

Table 3: DL data of DXM-loaded OBMD particles obtained with formulations DXM-**D**-0.1 characterized by different oligomer concentrations while maintaining the surfactant concentration constant at 0.1 wt.% and without the addition of a cosolvent to the organic phase. The value shown is the median of at least three batches with the corresponding range in brackets.

	DXM-0.5-0.1	DXM-1-0.1	DXM-1.5-0.1	DXM-2-0.1
DL (wt.%)	0.92 (0.67-1.61)	1.14 (0.91-1.33)	1.04 (0.81-1.14)	2.9 (1.7-3.3)

Influence of cosolvent addition

Cosolvents, such as acetone and ethanol, added to the organic phase can support solubilizing the payload, thus changing the formulation from a solid-in-oil-in-water to an oil-in-water dispersion. Cosolvents can affect the particle characteristics, for

example by reducing the particles size and increasing the DL [44-46], but may also support drug leakage to the continuous phase based on phase distribution coefficients. The influence of acetone as cosolvent on DXM encapsulation in particles from 1 wt.% OBMD was studied for two different surfactant concentrations. The addition of acetone to the formulation resulted in larger particles, with a direct correlation between the particle size and the amount of acetone used, when 0.1 wt.% sOEG-DAT was employed as stabilizer (Fig. 4a). The increase of particle size was less pronounced at higher surfactant concentration of 0.5 wt.% (Fig. 4b). This suggests that sOEG-DAT of 0.5 wt.% had a superior capability to stabilize the emulsion (see also Fig. 2), while lower surfactant concentration may allow tuning particle sizes from 590 nm (no acetone) to 750 nm and 1060 nm when an organic phase with 20 or 40 vol% of acetone were used, respectively. Also the polydispersity increased when acetone was added to the formulation, reaching a broad size distribution (PDI = 0.48) when 0.4 mL of acetone was used (DXM-1-0.1-40).

While the relationship between the oligomer or surfactant concentrations and OBMD particle dimension follows the trend described in literature [27,36,37], the reduction of particle sizes reported for different polyesters in presence of cosolvents [44,45] could not be observed in the case of OBMD, at least not at the lower surfactant concentration (0.1 wt.%). This highlights the importance of a systematic study in case of new matrix materials. A number of processes might potentially be involved in those increasing particle sizes. The diffusion of acetone out of the emulsified droplets might interfere with the droplet stabilization provided by the surfactant molecules, e.g. disrupt the surfactant layer, thus leading to the formation of bigger droplets and, therefore, larger particles. The cosolvent may also influence the surface tension between the two solvents or have an effect of the surfactant solubility in the water phase, thus affecting the capability of the surfactant to stabilize the emulsion. Furthermore, given the ability

of OBMD to act as hydrogen bond donor and acceptor, stronger interaction with acetone (compared to acetone with PLGA) might have altered the kinetics of acetone flux to the continuous phase, so that principles earlier described for cosolvent systems for hydrophobic copolyesters [44] may not be directly translated to OBMD.

The DL of the formulations with both 0.1 and 0.5 wt.% surfactant concentrations was changing only slightly with values between 0.8 and 1.1 wt.%, while the addition of a cosolvent to the formulation has been demonstrated to affect the DL in other systems including cases with a higher DL (see Table 4) [46-48]. The limited effect of acetone on DL of OBMD particles might indicate that the initial state of DXM (dispersed vs. dissolved) during particle preparation was not a main impact factor. This might be due to the diffusion of acetone into the aqueous phase with the result of a reduced solubility of the drug in the organic phase, which eventually contained DXM precipitated similar to acetone-free formulations. The only exception for the DL value was detected in the formulation performed with surfactant concentration of 0.1 wt.% and 40 Vol% of acetone in the organic phase (DXM-1-0.1-40): the DL values showed a large variability with the triplicates having DL of 1.9 up to 3 wt.%. However, the high polydispersity of this set of particles, which would likely result in a non-homogeneous biological distribution, together with the large variability of the particle DL makes this formulation less preferred for further evaluation as drug delivery systems.

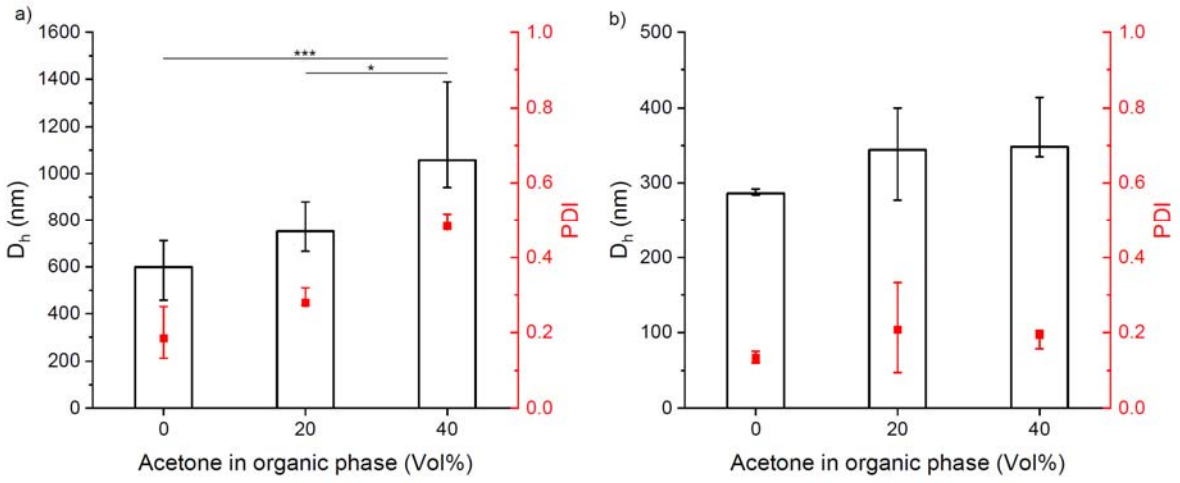

Fig. 4: DLS data of DXM-loaded OBMD particles obtained in dependency of the amount of acetone in the formulation as a cosolvent studied with surfactant concentrations of (a) 0.1 wt.% in formulations DXM-1-0.1-**C** and (b) 0.5 wt.% in formulations DXM-1-0.5-**C**. The median and range (error bars) of at least three batches are shown. Bars indicate statistically significant different values with * $p < 0.05$ and *** $p < 0.001$.

Table 4: DL data of DXM-loaded OBMD particles obtained in dependency of the amount of acetone in the formulation as a cosolvent studied with surfactant concentrations of 0.1 wt.% in formulations DXM-1-0.1-**C** and 0.5 wt.% in formulations DXM-1-0.5-**C**. The value shown is the median of at least three batches with corresponding range in brackets.

	DXM-1-0.1-0	DXM-1-0.1-20	DXM-1-0.1-40	DXM-1-0.5-0	DXM-1-0.5-20	DXM-1-0.5-40
DL (wt.%)	1.14 (0.91-1.33)	0.78 (0.66-0.8)	2.23 (1.87-3.00)	0.86 (0.83-1.06)	0.98 (0.87-1.33)	0.97 (0.82-1.06)

Influence of encapsulated molecule

The physicochemical properties of an encapsulated molecule may affect the particle size and the DL [62]. In order to investigate whether OBMD particle formation is influenced by the molecule embedded, unloaded (blank), DXM-loaded and NR-loaded carriers were prepared. Although DXM and NR have similar molar masses (M_{DXM} = 392.5 g·mol^{-1}; M_{NR} = 318.4 g·mol^{-1}), they differ in their octanol/water partition coefficient (Log P) (Log P_{DXM} = 1.83; Log P_{NR} = 3.5) and, in relation to it, their solubility

in water (solubility DXM at 25 °C = ~100 µg·mL^{-1} [63]; solubility NR < 1 µg·mL^{-1} [64]). The difference in aqueous solubility might play an important role in determining the DL and release kinetics of the two molecules.

Two different surfactant concentrations (0.1 and 0.5 wt.% sOEG-DAT) were explored to prepare unloaded, DXM-loaded and NR-loaded OBMD particles. The DL of NR-loaded particles was 0.8 wt.%, which is similar to the DL of DXM-loaded particles (Tab 5). As it is depicted in Fig. 5, the sizes of the unloaded, DXM- and NR- loaded particles were similar for the respective surfactant concentration. Again, with a D_h of 600-750 nm and a PDI of about 0.25, 0.1 wt.% sOEG-DAT resulted in larger and less homogeneously sized particles compared to 0.5 wt.% sOEG-DAT (D_h of 300-350 nm; PDI < 0.2). Statistical analysis performed using an one-way ANOVA test showed no significant difference between in the sizes of unloaded, DXM- and NR-loaded particles of a given formulation. This suggests that the particle preparation process was robust and not affected by the type of encapsulated compound.

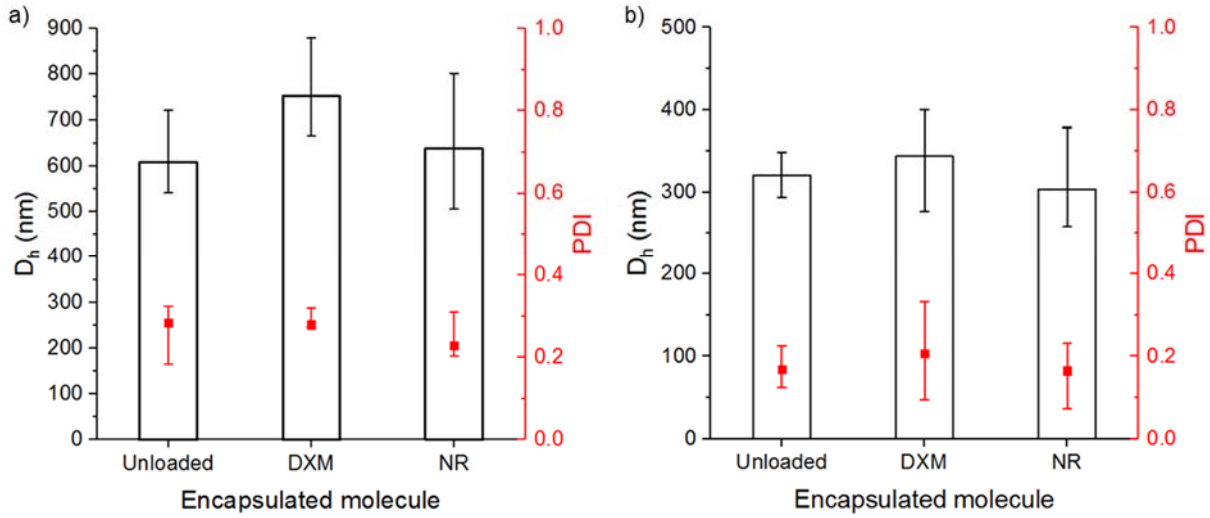

Fig. 5: DLS data comparing unloaded, DXM- and NR-loaded OBMD particles obtained at surfactant concentrations of (a) 0.1 wt.% in formulations **P**-1-0.1-20 and (b) 0.5 wt.% in formulations **P**-1-0.5-20. The median and range (error bars) of at least three batches are shown.

Table 5: DL data comparing DXM- and NR-loaded OBMD particles obtained at surfactant concentrations of 0.1 wt.% in formulations **P**-1-0.1-20 and 0.5 wt.% in formulations **P**-1-0.5-20. The value shown is the median of at least three batches and the corresponding range in brackets.

	DXM-1-0.1-20	NR-1-0.1-20	DXM-1-0.5-20	NR-1-0.5-20
DL (wt.%)	0.78 (0.66-0.8)	0.83 (0.67-0.91)	0.98 (0.87-1.33)	0.77 (0.57-1.17)

Release and *ex vivo* diffusion study

In order to evaluate the effect of particle size and of the physicochemical properties of the compound embedded in OBMD on the release behavior, *in vitro* release studies were performed at 32 °C, corresponding to the surface temperature of human skin [65]. Two sets of particle suspensions with a size of about 300 nm (DXM-1-0.1-20, NR-1-0.1-20) and about 600 nm (DXM-1-0.5-20, NR-1-0.5-20) with encapsulated DXM or NR have been selected.

The DXM release kinetics showed an initial burst release (55-60 wt.% in the first hour) with more than 90 wt.% of the encapsulated drug being released in 24 h (Fig. 6). The release kinetics were influenced by the particle sizes, though only to a small extent for DXM: the ~300 nm particles showed a slightly faster drug release compared to the ~600 nm particles. A high initial release is often observed for submicron particles due to the localization of a large quantity of drug close to or at the surface [66] and the relatively short diffusive pathway from the particle core to the particle surface. A similar burst release, in this case characterized by the release of almost 100 wt.% of the loaded DXM in 4 h, has been observed before for PLGA submicron particles [67]. A very fast drug release is desired in those applications that require the passage of a quantity of drug to reach the therapeutic dose, as in the case of wound healing [66] or angioplasty performed with drug-coated balloons [68].

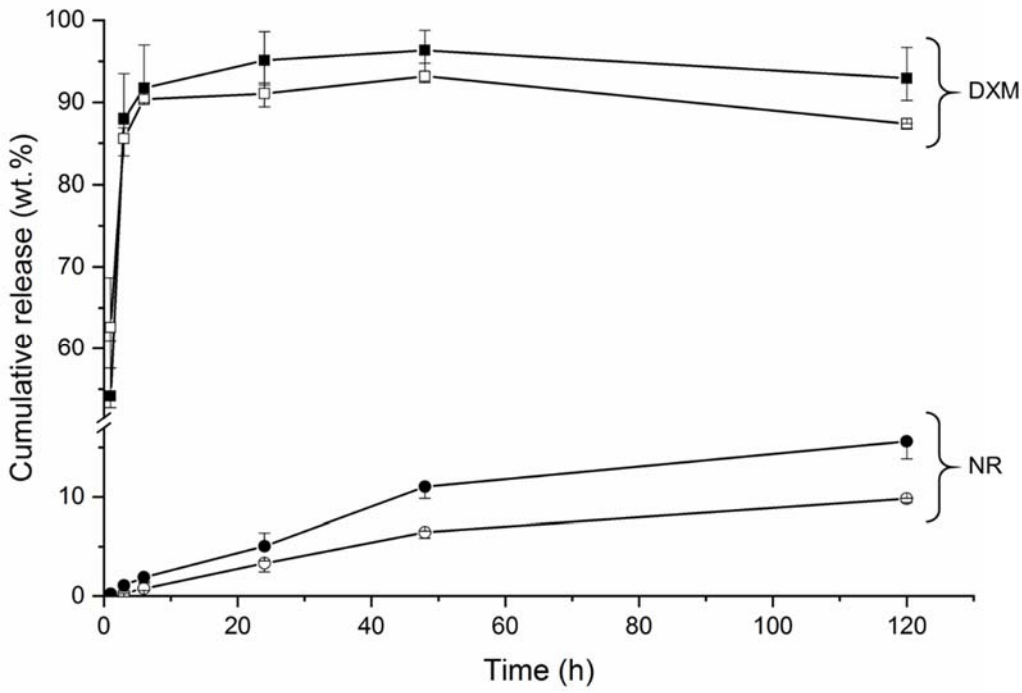

Fig. 6: *In vitro* release profiles in PBS buffer of DXM (□/■) and NR (○/●) depending on the OBMD particle size. DXM release data for 590 nm (□) and 340 nm (■) DXM-loaded OBMD particles from formulations DXM-1-0.1-20 and DXM-1-0.5-20, respectively. NR release data from 640 nm (○) and 320 nm (●) NR-loaded OBMD particles from formulations NR-1-0.1-20 and NR-1-0.5-20, respectively. Median and range are shown (n = 3).

The release of NR was slower compared to DXM (Fig. 6). This different behavior can be attributed to the lower solubility of NR in water. Also in the case of DXM- and NR-loaded particles prepared from block copolymers of poly(ethylene glycol) (PEG) and poly(ε-caprolactone) a much faster DXM release compared to the NR release has been reported, and has been attributed to stronger hydrophobicity of NR compared to DXM [69]. In the case of NR release, the particle size played a major role in the release kinetics compared to DXM-loaded particles. Indeed, ~16 wt.% of the loaded drug was released after 5 days in case of the ~300 nm particles, while only ~10 wt.% of NR was delivered when the particle size increased to ~600 nm, probably due to their higher surface to volume ratio.

The release profiles obtained with both DXM and NR were analyzed by employing various kinetic models: zero order, first order, Higuchi, Korsmeyer-Peppas and Hixon-

Crowell models [70] (Tab. S.1, supporting information). In the case of DXM release, the low values of the correlation coefficients obtained from the analysis (< 0.6) indicated that these models could not describe the drug release, suggesting that phase distribution of the drug or drug adsorption/desorption might be the determining release mechanisms rather than drug diffusion. The NR release pattern could much better be fitted by these models, as seen by correlation coefficients of generally > 0.9. For both particle sizes, high correlation coefficients (0.97) were obtained when the Higuchi model was applied, which may indicate that the release was mainly controlled by the diffusion of the dye through the particle matrix (Fig. 7). The high values of the release exponents of the Korsmeyer-Peppas equation with n > 0.85 suggested a super case II transport, i.e. drug release is not mainly controlled by a single event, like drug diffusion or polymer swelling, but it is rather influenced by many factors simultaneously. In this case, the presence of pores in some of the particles, the penetration of the release media into the carrier and the temperature at which the drug release is performed, which is close to the oligomer T_g in the presence of water ($T_{g,onset}$ = ~34 °C, [20]), might be some of the factors that influenced the release of the dye from these particles. The penetration of the release medium into the matrix, together with the temperature of the release media (32 °C), have possibly contributed to thermodynamic changes of the oligomer conformation, which can affect the diffusion of the drug through the matrix [71].

The lower correlation coefficients obtained when the Hixon-Crowell model was applied (< 0.94) suggest that the matrix does not degrade during the time frame used for the release studies (120 hours), as expected since also the OBMD films did not show evident mass change in 45 days in a previous study [20].

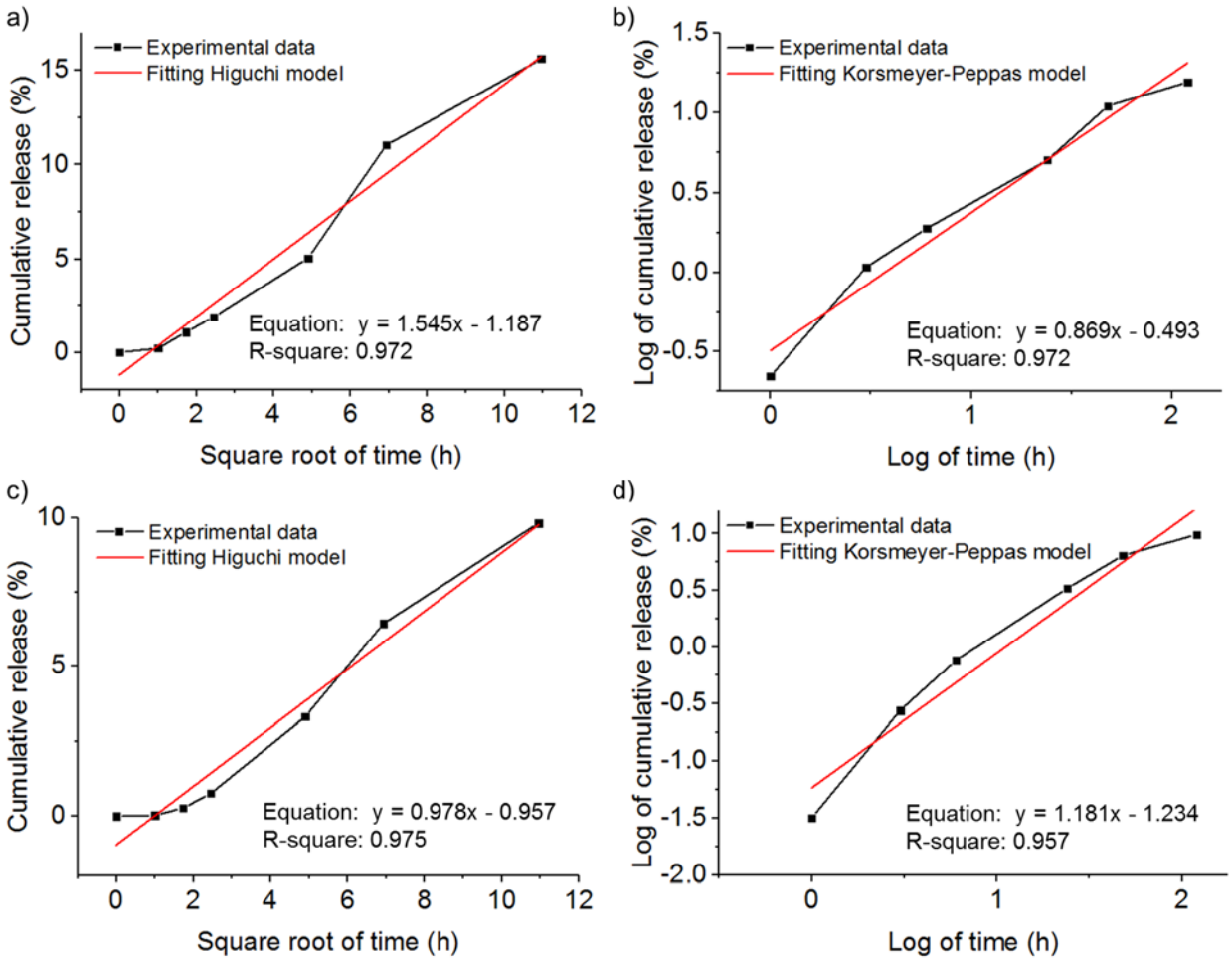

Fig. 7: Higuchi and Korsmeyer-Peppas models applied to the NR release from 300 nm (a and b) and 600 nm (c and d) OBMD particles. The kinetic models have been applied to the data depicted in Fig. 6. The medial value of the release curves of three different experiments for each formulation were used (n=3).

This analysis demonstrated that while the particle size was not affected by the loading of DXM or NR, the different physiochemical properties, especially the water solubility, of the two molecules had an evident effect on the release profile from the particles, similar to other systems [69]. While DXM showed a burst release, as already observed for other submicron carriers [67], the release of NR was slower and could be associated to the diffusion of the dye through the matrix and to the influence of other factors, e.g. the plasticizing effect of the water to the system [20].

With regards to the particle application for the treatment of skin disorders, the possibility of preparing drug- and dye-loaded particles of the same size allow to

investigate the therapeutic effect of the drug and to visualize the particle penetration through the tissue. Moreover, the DL achieved is similar to the DL of DXM-loaded polymeric particulate carriers that have been studied for skin and ocular delivery [58]. Concerns could be raised regarding the fast DXM release observed in this study, as this could result in the drug being released before the particles have reached their target. However, it has to be taken into consideration that the very little amount of fluid present in the skin and within the hair follicles is probably going to result in a slower DXM release compared to the one observed in this study, in which sink conditions where maintained. Indeed, non sink conditions, as in the case of the skin, are likely to lead to a slower kinetics than under sink conditions, especially in the case of fast releasing carriers [58,72]. Moreover, penetration studies on *ex vivo* skin samples are often performed in a time range of 30 min – 1 hour [3,50,51] and the release obtained here showed that 40 wt.% of the encapsulated drug is still in the particles after 1 hour. The first preliminary *ex vivo* follicular penetration studies to evaluate the capability of the OBMD particles to penetrate into the hair follicle have been performed by applying the NR-loaded particle suspension on porcine ear skin samples. Two different particle sizes of about 300 and 600 nm were investigated and compared to a NR-containing cream. The data suggested that with both particle sizes, NR was detected inside the hair follicles at an averaged depth of 260-270 µm (Fig. 8). However, a tendency of a deeper NR penetration up to 370-380 µm was observed in some of the replicates performed using the smaller particles. Moreover, the data obtained with the 260 nm particles were not significantly different compared to those obtained with the cream formulation containing NR. The slow and sustained release of the cargo is a potential benefit of the particles compared to the cream.

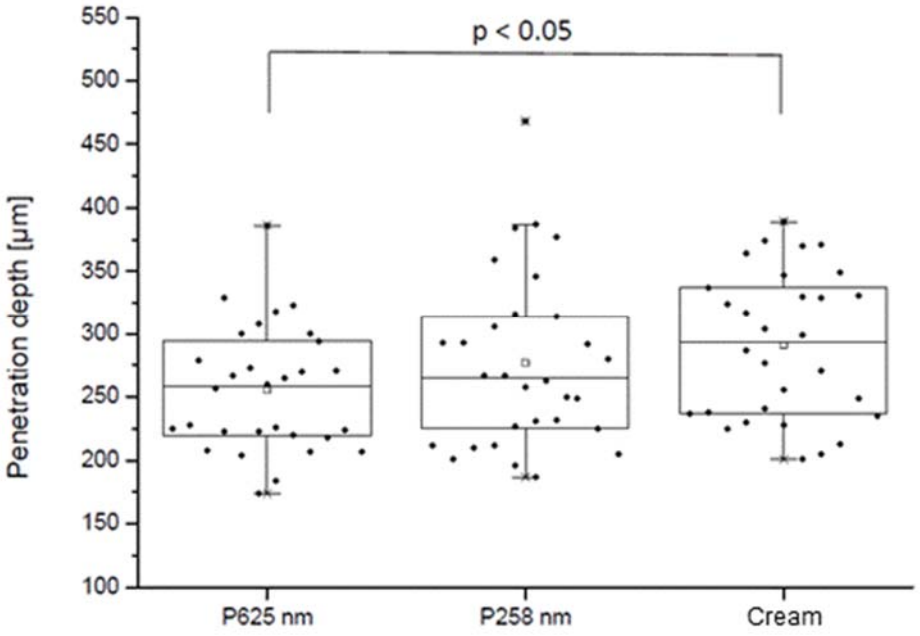

Fig. 8: Nile red (NR) penetration depth in hair follicles of porcine ear skin samples achieved by applying NR-loaded OBMD particles of 625 (formulation NR-1-0.1-20) and 258 nm (formulation NR-1-0.5-20) and a NR-containing cream.

While in the case of topical applications, e.g. skin or ocular delivery, the particles are unlikely to reach other tissues, attention has to be paid in case of a systemic administration. In that case, the risk related to the penetration of the particles and the delivery of the cargo into undesired compartments or organs, e.g. the liver or the brain, have to be carefully evaluated. Immunogenic effects of depsipeptide-based materials or their degradation products have to be evaluated in the future in *in vivo* models when developing the material system further in view of a specific application.

Conclusion

This study has shown that by using an emulsion solvent evaporation process and by varying different formulation parameters, the size of drug-loaded OBMD submicron particles can successfully be tailored in a size range between 300 and 950 nm while having a narrow size distribution. The trend encountered when increasing the oligomer

and surfactant concentration was similar to what has been detected with some polyester-based particulate systems. In addition, in this study the particle size range that was achieved was wider compared to most of the cases found in the literature, especially compared to the influence of the oligomer concentration on PLGA-based particle diameters. The addition of acetone to the formulation showed the opposite effect compared to what was detected for polyester-based particles, as in the case of OBMD particles, the addition of acetone resulted in an increase of the particle size, which may be related to the increased capability of OBMD to establish interactions with acetone compared to polyesters. The encapsulation of molecules having different physicochemical properties did not influence the particle size and polydispersity, but it affected the release profile. The release kinetics was mainly correlated with the water solubility of the two molecules, with DXM having a higher water solubility and thus showing a faster release.

The possibility of preparing OBMD submicron particle in a wide size range and having similar particle sizes even for molecules of different physicochemical properties enables the potential application of these particles for several clinical applications that require different drug carrier sizes, e.g. skin and ocular diseases. For instance, the antiinflammatory drug DXM and the dye NR encapsulated in this study are both relevant for skin delivery, since DXM is clinically used to treat inflammatory skin diseases while NR allows to follow the particles penetration in the tissue during application. Preliminary hair follicle penetration studies performed with NR-loaded particles of about 300 and 600 nm showed that NR could be visualized in the hair follicles of porcine ear skin samples. Whether the drug loading and release profile obtained in this study is sufficient to achieve a desired therapeutic effect will have to be shown in subsequent studies, as in the end not the drug loading but the transport efficacy will rule a therapeutic outcome. In the case a higher DL and a slower drug

release are desired, the introductions of different functionalities in the side chains in the ODPs could be investigated. Such functional groups could indeed enhance the interaction with the drug molecules by having multiple non-covalent bonds and, hence, result in a higher DL and sustained drug release.

Acknowledgment:

This work was financially supported by the Heltmoltz Association through programme-oriented funding and by the Deutsche Forschungsgemeinschaft (CRC 1112 “Nanocarriers”, project A03). H. Schmidt is acknowledged for technical support.

References:

[1] Vogt A, Wischke C, Neffe AT, Ma N, Alexiev U, Lendlein A. Nanocarriers for drug delivery into and through the skin — Do existing technologies match clinical challenges? J Controlled Release. 2016;242:3-15.
[2] Lademann J, Richter H, Schaefer UF, Blume-Peytavi U, Teichmann A, Otberg N, Sterry W. Hair follicles - a long-term reservoir for drug delivery. Skin Pharmacol Physiol. 2006;19(4):232-6.
[3] Patzelt A, Richter H, Knorr F, Schafer U, Lehr CM, Dahne L, Sterry W, et al. Selective follicular targeting by modification of the particle sizes. J Controlled Release. 2011;150(1):45-8.
[4] Mir M, Ahmed N, Rehman Au. Recent applications of PLGA based nanostructures in drug delivery. Colloids Surf, B. 2017;159:217-231.
[5] Diebold Y, Calonge M. Applications of nanoparticles in ophthalmology. Prog Retinal Eye Res. 2010;29(6):596-609.
[6] Fernandez Tena A, Casan Clara P. Deposition of inhaled particles in the lungs. Arch Bronconeumol. 2012;48(7):240-6.
[7] de Campos AM, Diebold Y, Carvalho EL, Sánchez A, Alonso MJ. Chitosan nanoparticles as new ocular drug delivery systems: in vitro stability, in vivo fate, and cellular toxicity. Pharm Res. 2004;21(5):803-10.
[8] Dubald M, Bourgeois S, Andrieu V, Fessi H. Ophthalmic Drug Delivery Systems for Antibiotherapy—A Review. Pharmaceutics. 2018;10(1):10.
[9] Almeida H, Amaral MH, Lobão PAL, Silva AC, Loboa JMS. Applications of polymeric and lipid nanoparticles in ophthalmic pharmaceutical formulations: present and future considerations. J Pharm Pharm Sci. 2014;17 3:278-93.
[10] Bachu RD, Chowdhury P, Al-Saedi ZHF, Karla PK, Boddu SHS. Ocular Drug Delivery Barriers-Role of Nanocarriers in the Treatment of Anterior Segment Ocular Diseases. Pharmaceutics. 2018;10(1):28.
[11] Janagam DR, Wu L, Lowe TL. Nanoparticles for drug delivery to the anterior segment of the eye. Adv Drug Delivery Rev. 2017;122:31-64.
[12] Imperiale JC, Acosta GB, Sosnik A. Polymer-based carriers for ophthalmic drug delivery. J Controlled Release. 2018;285:106-141.
[13] Weng Y, Liu J, Jin S, Guo W, Liang X, Hu Z. Nanotechnology-based strategies for treatment of ocular disease. Acta Pharm Sin B. 2017;7(3):281-291.
[14] Sandri G, Bonferoni MC, Ferrari F, Rossi S, Caramella C, The role of particle size in drug release and absorption. In: Merkus H, Meesters Gs, Editors. Particulate Products Particle Technology Series, Cham: Springer; 2014, p. 323-341.
[15] Danaei M, Dehghankhold M, Ataei S, Hasanzadeh Davarani F, Javanmard R, Dokhani A, Khorasani S, et al. Impact of Particle Size and Polydispersity Index on the Clinical Applications of Lipidic Nanocarrier Systems. Pharmaceutics. 2018;10(2):57.
[16] Matsumoto K, Mizukoshi K, Oyobikawa M, Ohshima H, Sakai Y, Tagami H. Objective evaluation of the efficacy of daily topical applications of cosmetics bases

using the hairless mouse model of atopic dermatitis. Skin Res Technol. 2005;11(3):209-217.
[17] Trautmann A, Akdis M, Schmid-Grendelmeier P, Disch R, Bröcker E-B, Blaser K, Akdis CA. Targeting keratinocyte apoptosis in the treatment of atopic dermatitis and allergic contact dermatitis. J Allergy Clin Immunol. 2001;108(5):839-846.
[18] Ohya Y, Matsunami H, Ouchi T. Cell growth on the porous sponges prepared from poly(depsipeptide-co-lactide) having various functional groups. J Biomater Sci, Polym Ed. 2004;15(1):111-23.
[19] Feng Y, Guo J. Biodegradable Polydepsipeptides. Int J Mol Sci. 2009;10(2):589-615.
[20] Brunacci N, Neffe AT, Wischke C, Naolou T, Nochel U, Lendlein A. Oligodepsipeptide (nano)carriers: Computational design and analysis of enhanced drug loading. J Controlled Release. 2019;301:146-156.
[21] Schädlich A, Kempe S, Mäder K. Non-invasive in vivo characterization of microclimate pH inside in situ forming PLGA implants using multispectral fluorescence imaging. J Controlled Release. 2014;179:52-62.
[22] Pagar KP, Sardar SM, Vavia PR. Novel L-Lactide-depsipeptide polymeric carrier for enhanced brain uptake of rivastigmine in treatment of Alzheimer's disease. J Biomed Nanotechnol. 2014;10(3):415-426.
[23] Ohya Y, Nakai T, Nagahama K, Ouchi T, Tanaka S, Kato K. The Synthesis and Biodegradability of Poly (lactide-random-depsipeptide)-PEGPoly (lactide-random-depsipeptide) ABA-type Triblock Copolymers. Journal of bioactive and compatible polymers. 2006;21(6):557-577.
[24] Wang W, Naolou T, Ma N, Deng Z, Xu X, Mansfeld U, Wischke C, et al. Polydepsipeptide Block-Stabilized Polyplexes for Efficient Transfection of Primary Human Cells. Biomacromolecules. 2017;18(11):3819-3833.
[25] Yan W, Fang L, Noechel U, Kratz K, Lendlein A. Influence of programming strain rates on the shape-memory performance of semicrystalline multiblock copolymers. J Polym Sci, Part B: Polym Phys. 2016;54(19):1935-1943.
[26] Feng Y, Lu J, Behl M, Lendlein A. Progress in depsipeptide-based biomaterials. Macromol Biosci. 2010;10(9):1008-21.
[27] Pagar K, Vavia P. Rivastigmine-loaded L-lactide-depsipeptide polymeric nanoparticles: decisive formulation variable optimization. Sci Pharm. 2013;81(3):865-85.
[28] Naolou T, Lendlein A, Neffe AT. Influence of metal softness on the metal-organic catalyzed polymerization of morpholin-2,5-diones to oligodepsipeptides. Eur Polym J. 2016;85:139-149.
[29] Dirauf M, Bandelli D, Weber C, Görls H, Gottschaldt M, Schubert US. TBD-Catalyzed Ring-Opening Polymerization of Alkyl-Substituted Morpholine-2,5-Dione Derivatives. Macromol Rapid Commun. 2018;39(23):1800433.
[30] Brunacci N, Wischke C, Naolou T, Neffe AT, Lendlein A. Influence of surfactants on depsipeptide submicron particle formation. Eur J Pharm Biopharm. 2017;116:61-65.
[31] Vanderhoff JW, El-Aasser MS, Ugelstad J, *Polymer emulsification process*, U.S. Patent 4,177,177., 1979.
[32] Desgouilles S, Vauthier C, Bazile D, Vacus J, Grossiord J-L, Veillard M, Couvreur P. The Design of Nanoparticles Obtained by Solvent Evaporation: A Comprehensive Study. Langmuir. 2003;19(22):9504-9510.
[33] Guerreiro LH, Da Silva D, Ricci-Junior E, Girard-Dias W, Mascarenhas CM, Sola-Penna M, Miranda K, et al. Polymeric particles for the controlled release of human amylin. Colloids Surf, B. 2012;94:101-106.
[34] Poletto FS, Fiel LA, Donida B, Ré MI, Guterres SS, Pohlmann AR. Controlling the size of poly(hydroxybutyrate-co-hydroxyvalerate) nanoparticles prepared by

emulsification–diffusion technique using ethanol as surface agent. Colloids Surf, A. 2008;324(1):105-112.
[35] Ahlin P, Kristl J, Kristl A, Vrečer F. Investigation of polymeric nanoparticles as carriers of enalaprilat for oral administration. Int J Pharm. 2002;239(1):113-120.
[36] Youm I, Murowchick JB, Youan B-BC. Entrapment and release kinetics of furosemide from pegylated nanocarriers. Colloids Surf, B. 2012;94:133-142.
[37] Esmaeili A, Saremnia B, Koohian A, Rezazadeh S. Mechanism of nanocapsules of Matricaria recutita L. extract formation by the emulsion–diffusion process. Superlattices Microstruct. 2011;50(4):340-349.
[38] Hoa LTM, Chi NT, Nguyen LH, Chien DM. Preparation and characterisation of nanoparticles containing ketoprofen and acrylic polymers prepared by emulsion solvent evaporation method. J Exp Nanosci. 2012;7:189 - 197.
[39] Lee SC, Oh JT, Jang MH, Chung SI. Quantitative analysis of polyvinyl alcohol on the surface of poly(d,l-lactide-co-glycolide) microparticles prepared by solvent evaporation method: effect of particle size and PVA concentration. J Controlled Release. 1999;59(2):123-132.
[40] Sahoo SK, Panyam J, Prabha S, Labhasetwar V. Residual polyvinyl alcohol associated with poly (d,l-lactide-co-glycolide) nanoparticles affects their physical properties and cellular uptake. J Controlled Release. 2002;82(1):105-114.
[41] Urbaniak T, Musiał W. Influence of solvent evaporation technique parameters on diameter of submicron lamivudine-poly-ε-caprolactone conjugate particles. Nanomaterials. 2019;9(9):1240.
[42] Scholes PD, Coombes AGA, Illum L, Daviz SS, Vert M, Davies MC. The preparation of sub-200 nm poly(lactide-co-glycolide) microspheres for site-specific drug delivery. J Controlled Release. 1993;25(1):145-153.
[43] Iqbal M, Valour J-P, Fessi H, Elaissari A. Preparation of biodegradable PCL particles via double emulsion evaporation method using ultrasound technique. Colloid Polym Sci. 2015;293(3):861-873.
[44] Maia JL, Santana MHA, Ré MI. The effect of some processing conditions on the characteristics of biodegradable microspheres obtained by an emulsion solvent evaporation process. Braz J Chem Eng. 2004;21:01-12.
[45] Liu J, Qiu Z, Wang S, Zhou L, Zhang S. A modified double-emulsion method for the preparation of daunorubicin-loaded polymeric nanoparticle with enhanced in vitro anti-tumor activity. Biomed Mater (Bristol, U K). 2010;5(6):065002.
[46] Rawat A, Burgess DJ. Effect of ethanol as a processing co-solvent on the PLGA microsphere characteristics. Int J Pharm. 2010;394(1-2):99-105.
[47] Yand Q, Reams R, Owusu-Ababio G. Effect of Solvent Composition During Preparation on the Characteristics of Enoxacin Microparticles. J Pharm Pharmacol. 1999;51(6):659-665.
[48] Sahana DK, Mittal G, Bhardwaj V, Kumar MNVR. PLGA Nanoparticles for Oral Delivery of Hydrophobic Drugs: Influence of Organic Solvent on Nanoparticle Formation and Release Behavior In Vitro and In Vivo Using Estradiol as a Model Drug. J Pharm Sci. 2008;97(4):1530-1542.
[49] Bodmeier R, McGinity JW. Solvent selection in the preparation of poly(dl-lactide) microspheres prepared by the solvent evaporation method. Int J Pharm. 1988;43(1):179-186.
[50] Mak WC, Patzelt A, Richter H, Renneberg R, Lai KK, Rühl E, Sterry W, et al. Triggering of drug release of particles in hair follicles. J Controlled Release. 2012;160(3):509-514.

[51] Patzelt A, Richter H, Dahne L, Walden P, Wiesmuller KH, Wank U, Sterry W, et al. Influence of the vehicle on the penetration of particles into hair follicles. Pharmaceutics. 2011;3(2):307-14.
[52] Julich-Gruner KK, Roch T, Ma N, Neffe AT, Lendlein A. Synthesis and characterization of star-shaped oligo(ethylene glycol) with tyrosine derived moieties under variation of their molecular weight. Clin Hemorheol Microcirc. 2015;60(1):13-23.
[53] Cooper DL, Harirforoosh S. Design and Optimization of PLGA-Based Diclofenac Loaded Nanoparticles. PLoS ONE. 2014;9(1):e87326.
[54] Adebileje T, Valizadeh A, Amani A. Effect of formulation parameters on the size of PLGA nanoparticles encapsulating bovine serum albumin: a response surface methodology. J Contemp Med Sci. 2017;3(12).
[55] Kızılbey K. Optimization of rutin-loaded PLGA nanoparticles synthesized by single-emulsion solvent evaporation method. ACS Omega. 2019;4(1):555-562.
[56] Lemos-Senna E, Wouessidjewe D, Lesieur S, Duchêne D. Preparation of amphiphilic cyclodextrin nanospheres using the emulsification solvent evaporation method. Influence of the surfactant on preparation and hydrophobic drug loading. Int J Pharm. 1998;170(1):119-128.
[57] Su Z, Sun F, Shi Y, Jiang C, Meng Q, Teng L, Li Y. Effects of formulation parameters on encapsulation efficiency and release behavior of risperidone poly(D,L-lactide-co-glycolide) microsphere. Chem Pharm Bull. 2009;57(11):1251-6.
[58] Balzus B, Sahle FF, Hönzke S, Gerecke C, Schumacher F, Hedtrich S, Kleuser B, et al. Formulation and ex vivo evaluation of polymeric nanoparticles for controlled delivery of corticosteroids to the skin and the corneal epithelium. Eur J Pharm Biopharm. 2017;115:122-130.
[59] Sharma N, Madan P, Lin S. Effect of process and formulation variables on the preparation of parenteral paclitaxel-loaded biodegradable polymeric nanoparticles: A co-surfactant study. Asian J Pharm Sci. 2016;11(3):404-416.
[60] Operti MC, Fecher D, van Dinther EAW, Grimm S, Jaber R, Figdor CG, Tagit O. A comparative assessment of continuous production techniques to generate sub-micron size PLGA particles. Int J Pharm. 2018;550(1-2):140-148.
[61] Hernández-Giottonini KY, Rodríguez-Córdova RJ, Gutiérrez-Valenzuela CA, Peñuñuri-Miranda O, Zavala-Rivera P, Guerrero-Germán P, Lucero-Acuña A. PLGA nanoparticle preparations by emulsification and nanoprecipitation techniques: effects of formulation parameters. RSC Adv. 2020;10(8):4218-4231.
[62] Barichello JM, Morishita M, Takayama K, Nagai T. Encapsulation of Hydrophilic and Lipophilic Drugs in PLGA Nanoparticles by the Nanoprecipitation Method. Drug Dev Ind Pharm. 1999;25(4):471-476.
[63] Guillory JK. Handbook of Aqueous Solubility Data By Samuel H. Yalkowsky and Yan He. CRC Press, Boca Raton, FL. J Med Chem. 2003;46(19):4213-4213.
[64] Greenspan P, Fowler SD. Spectrofluorometric studies of the lipid probe, nile red. J Lipid Res. 1985;26(7):781-9.
[65] Raber AS, Mittal A, Schafer J, Bakowsky U, Reichrath J, Vogt T, Schaefer UF, et al. Quantification of nanoparticle uptake into hair follicles in pig ear and human forearm. J Controlled Release. 2014;179:25-32.
[66] Huang X, Brazel CS. On the importance and mechanisms of burst release in matrix-controlled drug delivery systems. J Controlled Release. 2001;73(2–3):121-136.
[67] Gomez-Gaete C, Tsapis N, Besnard M, Bochot A, Fattal E. Encapsulation of dexamethasone into biodegradable polymeric nanoparticles. Int J Pharm. 2007;331(2):153-9.

[68] Ramakrishna CD, Dave BA, Kothavade PS, Joshi KJ, Thakkar AS. Basic Concepts and Clinical Outcomes of Drug-Eluting Balloons for Treatment of Coronary Artery Disease: An Overview. J Clin Diagn Res. 2017;11(6):OE01-OE04.
[69] Krishnan V, Xu X, Barwe SP, Yang X, Czymmek K, Waldman SA, Mason RW, et al. Dexamethasone-loaded block copolymer nanoparticles induce leukemia cell death and enhance therapeutic efficacy: a novel application in pediatric nanomedicine. Mol Pharmaceutics. 2013;10(6):2199-210.
[70] Costa P, Sousa Lobo JM. Modeling and comparison of dissolution profiles. Eur J Pharm Sci. 2001;13(2):123-133.
[71] Rehage G, Ernst O, Fuhrmann J. Fickian and non-Fickian diffusion in high polymer systems. Discuss Faraday Soc. 1970;49(0):208-221.
[72] Liu P, De Wulf O, Laru J, Heikkilä T, van Veen B, Kiesvaara J, Hirvonen J, et al. Dissolution studies of poorly soluble drug nanosuspensions in non-sink conditions. AAPS PharmSciTech. 2013;14(2):748-756.

Supporting information

Table S.1: Equations and correlation coefficients obtained when applying different kinetic models to the release profile obtained from the NR-loaded OBMD particles of ~300 nm (NR-1-0.5-20) and ~600 nm (NR-1-0.1-20).

Model	~300 nm NR-loaded OBMD particle	~600 nm NR-loaded OBMD particle
Zero order	y = 0.133x + 1.142 R^2 = 0.920	y = 0.0849x + 0.499 R^2 = 0.935
First order	y = -0.001x + 1.995 R^2 = 0.929	y = -4E-04x + 1.998 R^2 = 0.941
Higuchi	y = 1.545x - 1.187 R^2 = 0.972	y = 0.978x - 0.957 R^2 = 0.974
Korsmeyer-Peppas	y = 0.869x - 0.493 R^2 = 0.9716	y = 1.181x - 1.234 R^2 = 0.957
Hixon-Crowell	y = 0.002x + 0.018 R^2 = 0.926	y = 0.001x + 0.008 R^2 = 0.939